

## ONLINE DATA SUPPLEMENTS

### **HIF-1 $\alpha$ in vascular smooth muscle regulates blood pressure homeostasis through a PPAR $\gamma$ -angiotensin II receptor type 1 (ATR1) axis**

**\*Yan Huang<sup>1,2</sup>, \*Annarita Di Lorenzo<sup>4</sup>, Weidong Jiang<sup>1,2</sup>, Anna Cantalupo<sup>4,5</sup>, William C. Sessa<sup>2,3</sup>, and Frank J. Giordano<sup>1,2</sup>.**

<sup>1</sup>Section of Cardiovascular Medicine, Department of Internal Medicine, and  
<sup>2</sup>Vascular Biology and Therapeutic Program, <sup>3</sup>Department of Pharmacology, Yale University School of Medicine, New Haven, CT, 06520, USA, <sup>4</sup>Department of Pathology and Laboratory Medicine, Weill Medical College of Cornell University, New York, NY, USA <sup>5</sup>Department of Pharmacology, University of Naples “Federico II”, Naples, Italy.

#### **Supplemental Material and Methods**

**Mean arterial blood pressure (MBP) response to AngII.** Male mice were anesthetized with ketamine/xylazine (100 and 5 mg/Kg of body weight, respectively). Trachea was orally intubated and connected to a volume-controlled ventilation at a respiratory rate of 100 breaths/min with a room air. A 1.4 French transducer-tipped catheter (Millar Inc., Houston, TX) was inserted into the ascending aorta via the right carotid artery to monitor the MBP recorded at 1,000 Hz (Powerlab, ADInstruments). AngII solution was infused via the left jugular vein at graded doses (0.125, 0.25, 0.5 and 1  $\mu$ g/kg body weight), each for 3 min. MBP was calculated with Chart 5 (ADInstruments).

**Echocardiographic studies.** Cardiac dimensions and function were analyzed by echocardiography using a Vevo 770 console (VisualSonics, Toronto, Canada) as previously described<sup>1,2</sup>. Mice were lightly anesthetized with inhaled isoflurane (0.2 % in O<sub>2</sub>). All measurements were obtained from three to six consecutive cardiac cycles, and the averaged values used for analysis. Left LV end-diastolic (LVDd), end-systolic (LVDs) dimensions, thickness of the interventricular septum (IVS) and posterior wall (PW) were measured from the M-mode tracings, and fractional shortening (FS) was calculated as [(LVDd – LVDs)/LVDd x100]. Diastolic measurements were performed using the leading-edge method of the American Society of Echocardiography<sup>1</sup>.

**Vascular reactivity ex-vivo.** Mice were sacrificed and the mesentery was rapidly removed and dissected in ice-cold Krebs solution (mM: 119 NaCl, 4.7 KCl, 2.5 CaCl<sub>2</sub>, 1 MgCl<sub>2</sub>, 25 NaHCO<sub>3</sub>, 1.2 KH<sub>2</sub>PO<sub>4</sub>, and 11 D-glucose). Mesenteric artery rings were mounted in a Multi Myograph System (Danish Myo Technology A/S, Denmark) and changes in arterial tone were recorded. High K<sup>+</sup> (60 mM) was used to induce steady blood vessel tone and until the magnitude of contractility response was reproducible. Cumulative concentration response curves to PE, 5-HT (10 nM to 30 μM) and AngII (0.1 nM to 1 μM) were performed to evaluate the contractility response. To evaluate tissue vasorelaxation and the integrity of the endothelium layer, cumulative concentration response curve to acetylcholine (Ach) (10 nM to 30 μM), and isoprotenerol (Isop) (10 nM to 30 μM) were performed on PE (1 μM) precontracted rings.

**Quantitative RT-PCR analyses.** Samples from aorta, VSMC, heart, lung, kidney and blood were homogenized with TRizol reagent (Invitrogen). Total RNA was isolated with the RNAEasy kit (Qiagen) and transcribed into complementary DNA with the use of the TaqMan protocol (Applied Biosystem). Quantitative PCRs were carried out using iCycler (Biorad) with specific primers against the genes of interest, SYBRgreen (Biorad) ready mix.

**Adenovirus infection and siRNA transfection.** Human aorta VSMC (hVSMC) between passage 3 and 6, were transfected with control or PPAR<sub>γ</sub> siRNA (Santa Cruz; 50nM). After 48h cells were treated with rosiglitazone (50μM; 12h) and cell lysates were subjected to WB analysis. In another set of experiments, control and PPAR<sub>γ</sub> siRNA treated hVSMC were infected with recombinant adenovirus encoding HIF-1 $\alpha$  (Ad-HIF1 $\alpha$ ) or control (Ad-ctr) at MOI 1:300 for 48h<sup>3</sup>. Cell lysates were analyzed by WB.

**Western Blot Analysis (WB).** Mouse thoracic aortas were snap frozen and pulverized in liquid nitrogen. Protein lysates were analyzed by SDS-polyacrylamide gel electrophoresis (PAGE) and immunoblotting as previously described<sup>4</sup>. Primary antibodies used include the following: against ATR1 (Santa Cruz Biotechnology), heat shock protein (Hsp90) (BD Transduction Laboratories),  $\beta$ -actin (Sigma), MAPK and phospho-MAPK (Cell Signaling); secondary fluorescence-labeled antibodies (LI-COR Biotechnology). Bands were visualized with the Odyssey Infrared Imaging System (LI-COR Biotechnology).

**Statistical analysis.** Data are expressed as mean $\pm$ s.e.m. The level of statistical significance was determined by ANOVA followed by Bonferroni's t-test for

multiple comparisons, or student t test using the GraphPad (San Diego) Prism software.

1. Boucher P, Gotthardt M, Li WP, Anderson RG, Herz J. Lrp: Role in vascular wall integrity and protection from atherosclerosis. *Science*. 2003;300:329-332
2. Savoia C, Touyz RM, Volpe M, Schiffrin EL. Angiotensin type 2 receptor in resistance arteries of type 2 diabetic hypertensive patients. *Hypertension*. 2007;49:341-346.
3. Carmeliet P, Dor Y, Herbert JM, Fukumura D, Brusselmans K, Dewerchin M, Neeman M, Bono F, Abramovitch R, Maxwell P, Koch CJ, Ratcliffe P, Moons L, Jain RK, Collen D, Keshert E. Role of hif-1alpha in hypoxia-mediated apoptosis, cell proliferation and tumour angiogenesis. *Nature*. 1998;394:485-490.
4. Lee SH, Wolf PL, Escudero R, Deutsch R, Jamieson SW, Thistlethwaite PA. Early expression of angiogenesis factors in acute myocardial ischemia and infarction. *N Engl J Med*. 2000;342:626-633.

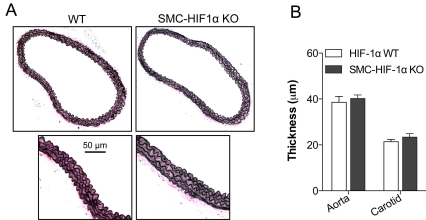


**Figure S1. The lack of HIF-1 $\alpha$  in VSMC did not alter aorta and carotid wall thickness.** (A) Elastica van Gieson staining of thoracic aorta cross-sections (scale bar, 50  $\mu\text{m}$ ), and (B) quantification of aorta and carotid wall thickness.



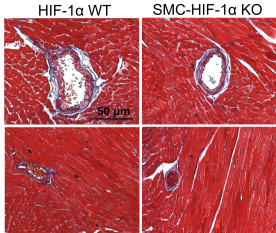


**Figure S2. SMC-HIF-1 $\alpha$ -KO mice did not show any difference in heart fibrosis compared to HIF-1 $\alpha$ -WT. Trichrome staining of SMC-HIF-1 $\alpha$ -KO and HIF-1 $\alpha$ -WT heart cross-sections. Scale bar, 50  $\mu$ m.**

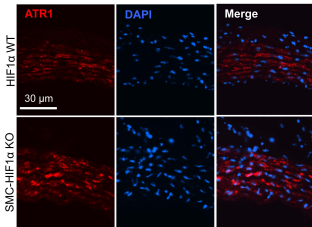


**Figure S3. ATR1 was increased in SMC-HIF-1 $\alpha$  KO aorta.** Representative immunofluorescent staining of HIF-1 $\alpha$  WT and SMC-HIF-1 $\alpha$  KO thoracic aorta cross-sections for ATR1 (red) and DAPI (blue). Scale bar, 50  $\mu$ m.

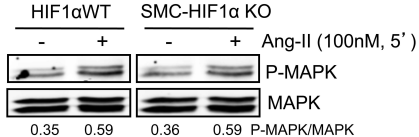


**Figure S4. The absence of HIF-1 $\alpha$  in VSMC did not affect Ang-II-induced MAPK activation.** Western blot analysis for P-MAPK and MAPK on quiescent HIF-1 $\alpha$  WT and SMC-HIF-1 $\alpha$  KO VSMC stimulated with Ang-II (100 nM; 5 min).

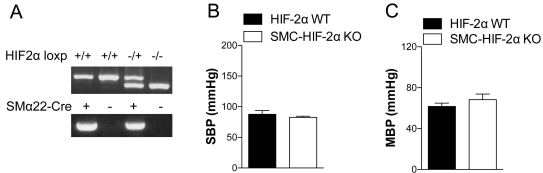


**Figure S5. HIF-2 $\alpha$  deletion from VSMC does not alter blood pressure.** (A) PCR demonstrating the genotypes obtained using SM22 $\alpha$ -Cre mice to delete HIF-2 $\alpha$  from smooth muscle. HIF-2 $\alpha$  floxed mice were obtained by Jackson Labs (cat. 009674). Hemodynamic parameters, (B) SBP and (C) MBP were measured with a Millar catheter in right carotid artery. n=6 per group, Student's T test was performed.

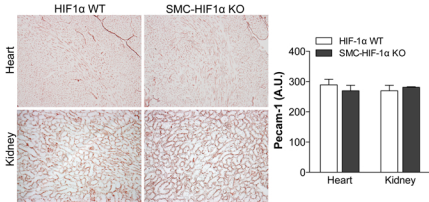


**Figure S6. Deletion of HIF-1 $\alpha$  from VSMC did not alter vascular density and morphology in heart and kidney.** (A) Anti-PECAM staining and (B) quantification revealed no significant changes in vascular density in any tissue studied (brain, lung, liver, heart, kidney evaluated; results from heart and kidney shown).